BOREAL ENVIRONMENT RESEARCH 20: 151–171
ISSN 1239-6095 (print) ISSN 1797-2469 (online)

Helsinki 30 April 2015

A semi-empirical model of boreal-forest gross primary production, evapotranspiration, and soil water — calibration and sensitivity analysis

Mikko Peltoniemi[1)2)]*, Minna Pulkkinen[2)], Mika Aurela[3)], Jukka Pumpanen[2)], Pasi Kolari[4)] and Annikki Mäkelä[2)]

[1)] *Finnish Forest Research Institute, P.O. Box 18, FI-01301 Vantaa, Finland (*corresponding author's e-mail: mikko.peltoniemi@metla.fi)*
[2)] *Department of Forest Sciences, P.O. Box 27, FI-00014 University of Helsinki, Finland*
[3)] *Finnish Meteorological Institute, P.O. Box 503, FI-00101 Helsinki, Finland*
[4)] *Department of Physics, P.O. Box 64, FI-00014 University of Helsinki, Finland*

Received 25 Oct. 2013, final version received 27 Oct. 2014, accepted 3 Oct. 2014

Peltoniemi M., Pulkkinen M., Aurela M., Pumpanen J., Kolari P. & Mäkelä A. 2015: A semi-empirical model of boreal-forest gross primary production, evapotranspiration, and soil water — calibration and sensitivity analysis. *Boreal Env. Res.* 20: 151–171.

Simple approaches to predicting ecosystem fluxes are useful in large-scale applications because existing data rarely support justified use of complex models. We developed a model of daily ecosystem gross primary production (P), evapotranspiration (E), and soil water content (θ), which only requires standard weather data and information about the fraction of absorbed radiation. We estimated the parameters of the model for two boreal Scots pine eddy-covariance sites (Hyytiälä and Sodankylä). The model predicted P and E adequately for Hyytiälä for both calibration and additional test years. The model calibrated for Hyytiälä slightly overestimated P and E in Sodankylä, but its performance levelled with the model calibrated for Sodankylä in a dry year. Sensitivity analysis of the model implied that drought prediction is sensitive, not only to key E submodel parameters, but also to P submodel parameters. Further improvement and calibrations of the model could benefit from forest sites with varying canopy and different species structures.

Introduction

When predicting the photosynthetic productivity of boreal forest ecosystems, availability of water from the soil has rarely been in focus due to humidity of the boreal climate (e.g. Bergh *et al*. 2003). However, climate change is predicted to alter the situation, because increasing summer temperatures will increase evaporation, which will not be fully compensated by summer precipitation, partially because variability of summer rains is expected to increase (IPCC 2007, Jylhä *et al*. 2009). Because of the small variability of rainfall in the boreal zone in the past, forests may be vulnerable to the increasing rainfall variability. It is therefore important to also include the effects of water availability in predictions of gross primary production (P). This requires a water balance model with linkages to stomatal conductance.

Detailed mechanistic water-balance models have been developed for boreal forests, where

Editor in charge of this article: Eero Nikinmaa

the soil is considered a layered system, and soil physics is described, including soil temperature distribution and its interaction with water content, plant water uptake, transpiration and evaporation at sub-daily time steps (e.g. Jansson and Moon 2001, Lauren *et al*. 2005). These models typically use the Penman-Monteith equation for canopy evapotranspiration (Monteith 1965), where the bulk canopy conductance is a combination of aerodynamic conductance and stomatal conductance, regulated by environmental factors through a big-leaf stomatal-conductance model. The stomatal conductance component is commonly modelled in relation to photosynthetic activity, either using multiplicative environmental modifiers (Bartlett *et al*. 2003, Jarvis 1976, Whitehead 1998) or the Ball-Berry-Leuning-type stomatal conductance (Leuning 1995) which is coupled with a Farquhar-type (Farquhar *et al*. 1980) photosynthesis model.

While the mechanistic approaches allow for detailed analyses of the water and carbon balances at specific sites, they require rather detailed and site-specific input data (e.g. soil variables) that are not easily transferable from one site to another (e.g. Wu *et al*. 2011). This mechanistic approach also requires high temporal resolution due to the non-linear response to driving variables, which makes aggregation to diurnal or longer scale complex (Phillips and Oren 1998). For purposes of large-scale regional analysis, therefore, a commonly used approach is to apply simplified models of potential evapotranspiration (PET), defined at daily to monthly time steps, and scale these down to actual evapotranspiration on the basis of the availability of water in the soil and vegetation cover over the same period, which itself is influenced by the evapotranspiration estimate. Commonly used PET models include the Thornthwaite (Thorthwaite 1948) and Hamon (Hamon 1963) models based on temperature, the Turc (Turc 1961) model based on global radiation, and the Priestley and Taylor (Priestley and Taylor 1972) model based on net radiation. However, these methods have been shown to produce different results that do not necessarily correlate well with actual evapotranspiration (Lu *et al*. 2005). The temperature-based methods have also been suggested to overestimate the increase in PET under climate change because the changes in temperature do not properly reflect the changes in net radiation that is a fundamental driver of PET (Shaw and Riha 2011). This may also lead to weaker transferability of such models from one biome or geographic area to another.

The expanding eddy-covariance measurement network has considerably increased our knowledge about ecosystem gas exchange (Baldocchi 2014) and it provides data to test the different approaches and to calibrate and fit models to empirical data. This could provide an opportunity to develop an intermediate model between the highly mechanistic, high-resolution models and the simple, index-type models based on PET and water availability. Interestingly in this respect, a recent comprehensive study of evapotranspiration of 12 Canadian eddy-flux sites of different vegetation types found that in the five boreal coniferous sites of the study, the so-called decoupling term (Ω) of the Penman-Monteith equation had values < 0.2, indicating that the stomatal conductance term was the key determinant of the actual evapotranspiration, as compared with the aerodynamic conductance (Brümmer *et al*. 2012). This corroborates the earlier analyses (Jarvis 1976, Kelliher *et al*. 1993) that modelling stomatal conductance is the key to estimating evapotranspiration at least from boreal coniferous forest canopies, while the aerodynamic conductance with its dependence, e.g., on wind speed appears to play a lesser role on average in these forests that are well-coupled to the atmosphere.

In this study, our objective was to develop a semi-empirical, intermediate-complexity model of evapotranspiration and its coupling with canopy photosynthesis, on the basis of eddy-flux and soil-moisture data. We used flux data from two eddy-flux sites in Finland, Hyytiälä (Suni *et al*. 2003) and Sodankylä (Aurela 2005, Thum *et al*. 2008). In addition, we had soil moisture and catchment drainage data from Hyytiälä. The Hyytiälä forest is one of the rare eddy-covariance sites where determination of drainage is possible and is regarded accurate. The Hyytiälä site is located on forest soil with a soil pool of known volume, from which water drains via a single exit channel (Ilvesniemi *et al*. 2010). The catchment water balance thus provides an

independent estimate of evapotranspiration that can be compared to evapotranspiration of the footprint area of the flux measurements.

Material and methods

Hyytiälä SMEAR II site

The Station for Measuring Ecosystem–Atmosphere Relations (SMEAR II) is a highly instrumented field-site located in a Scots-pine-dominated forest surrounding a 124 m tall measuring tower in Hyytiälä (southern Finland; 61°50.845N, 24°17.686E, 181 m a.s.l.) (Hari and Kulmala 2005). The mean temperature and precipitation in 1960–1990 were 3.8 °C and 709 mm, respectively. Topsoil is frozen during winter but melts completely by May, freezing again in December at the earliest. In 2006, the mean height of the stand within the 200-m radius from the measuring tower was 14.8 meters, the mean diameter at breast height (dbh) was 13.4 cm, and the number of trees 1440 ha^{-1} (trees > 5 cm dbh) (Ilvesniemi *et al*. 2009). Leaf area index (all-sided) of the stand varied between 6.7 and 8.4 in the years 1995–2008, being highest before thinning in 2002 and lowest after the thinning, and that of the ground vegetation was 2.9 and 2.8 in 2006 and 2008, respectively (Ilvesniemi *et al*. 2009).

At SMEAR II, two mini-catchments with known borders have been isolated on the top of the hill next to the measuring tower. On the down-slope side of the catchments two weirs were cast to the bedrock using watertight concrete. Each catchment is an independent hydrological unit that receives water from precipitation and water drains through the weirs only (Ilvesniemi *et al*. 2010). Here, we used the data from the larger catchment C1 (889 m^2).

The soil of the catchment consists of haplic podzol formed on glacial till, with average organic layer thickness of 5 cm. The soil volume (by layer) estimate is based on radar measurements conducted in 1 m × 1 m grid (Ilvesniemi *et al*. 2010). Using these measurements, we estimated that the effective depth of the soil in terms of soil water dynamics is 413 mm, i.e. the depth excluding stones and bedrock.

Soil water content (θ) at the site was measured using time domain reflectometry (TDR). The probes were installed in each soil horizon in the vertical face of five soil pits in the catchment.

For the purposes of this study, we defined the effective field capacity θ_{FC} of the site as the level at which soil water stabilizes after snowmelt and large rainfall events. The effective wilting point θ_{WP} was determined from the data as the lowest level of soil water reached, only allowing marginal changes in θ below θ_{WP}. As we determined θ_{WP} from the soil water data, it represents the lower limit of water during the years 1998–2012, and it does not imply a large degree of mortality in a forest.

The catchment and the measurements and instrumentation related to water balance are reported in detail elsewhere (Ilvesniemi *et al*. 2010).

Sodankylä northern boreal pine site

Sodankylä Scots pine forest is located in northern Finland (67°21.712N, 26°38.270E, elevation 179 m a.s.l.). The long-term (1981–2010) mean temperature and precipitation at the area are –0.4 °C and 527 mm, respectively (Pirinen *et al*. 2012). The ground is typically covered by snow from October until mid-May, and the uppermost soil layers are frozen during winter (Aurela 2005, Thum *et al*. 2008). The Scots pine stand (mean tree height of 13 m and tree density 2100 ha^{-1}) is located on fluvial sandy podzol. The soil consists of till (91%), sand, clay and stones. Soil is deeper than the root and fine-root layers (40–50 cm), with some large trees having pole root extending down to 3 m (T. Penttilä pers. comm.). The forest has regenerated naturally after forest fires. The age of trees is typically > 50 years with the average age being 100 years. The sparse ground vegetation consists of lichens (73%), mosses (12%) and ericaceous shrubs (15%).

Eddy-covariance and measurements of CO_2 and evapotranspiration fluxes

The CO_2 fluxes were measured using the micro-

meteorological eddy-covariance (EC) method which gives us direct measurements of CO_2 fluxes averaged at an ecosystem scale. In the EC method, the vertical CO_2 flux is obtained as the covariance of the high frequency (10 Hz) measurements of vertical wind speed and the CO_2 concentration (Baldocchi 2003). The EC instrumentation in Hyytiälä consisted of a Solent 1012R3 three-axis sonic anemometer (Gill Instruments Ltd., Lymington, UK) and a LI-6262 closed-path CO_2/H_2O gas analyser (Li-Cor Inc., Lincoln, NE, USA). In Sodankylä, a USA-1 (METEK GmbH, Elmshorn, Germany) anemometer and a LI-7000 (Li-Cor., Inc., Lincoln, NE, USA) closed path analyser were used. The EC fluxes were calculated as half-hourly averages taking into account the required corrections. The measurement systems and the post-processing procedures are presented in greater detail in Kolari *et al*. (2004) and Mammarella *et al*. (2009) for Hyytiälä, and in Aurela (2005) and Aurela *et al*. (2009) for Sodankylä.

In this study, we used daily estimates of P and E fluxes obtained from the EC data. The data from the Hyytiälä site were used for model parameterization, while those from the Sodankylä site were mainly used in testing of the model.

Daily totals of ecosystem P (g C m^{-2}) were obtained from half-hourly estimates, which were calculated as the difference between measured net ecosystem exchange (NEE) and modelled total ecosystem respiration (TER). Half-hourly TER was parameterised as a function of soil organic-layer temperature using the NEE data for nighttime when there is no P component and NEE equals TER. This dependence of nighttime TER on temperature was then extrapolated to daytime to obtain the full diurnal cycle. Before these computations, half-hourly NEE was filtered with site-specific criteria for turbulence and atmospheric stability. For Sodankylä, the daily values were obtained from the CarboEuropeIP database (Moffat *et al*. 2007, Papale *et al*. 2006, Reichstein *et al*. 2005). The data for Hyytiälä were calculated using our own programme utilizing practically the same procedures as those for Sodankylä (Kolari *et al*. 2009).

For fitting the model, we required that at least 70% of the half-hourly estimates of P, evapotranspiration (E), photosynthetic photoflux density (ϕ), vapour pressure deficit of atmosphere (D) and air temperature (T) are not gap-filled, otherwise the day was excluded from the fit, to avoid additional errors and correlations in data, which could be generated because of gap-filling. Days with $T < -10$ °C were excluded based on uncertainty of E flux measurements. Soil water measurements between December and April were discarded from the fit due to evidently low values generated by frost in the TDR measurements. This has presumably, a marginal effect on the model fit as E is not constrained by soil water during winter. Additionally, no soil-water measurements from between 1 April 2003 and 31 April 2005 were used in the model fitting.

The fraction of absorbed photosynthetic photon-flux density ($f_{a\phi}$) was estimated from annual estimates of leaf area (L_A) using the Lambert-Beer law and all-sided canopy leaf area, and the previously estimated site-specific extinction coefficient of 0.27 for Hyytiälä (Duursma and Mäkelä 2007). For Hyytiälä, measured yearly time series of L_A, including ground vegetation was used. For Sodankylä, a fixed estimate of $f_{a\phi}$ = 0.6 was used (Mäkelä *et al*. 2008). Seasonal variation in L_A in these coniferous stands was not accounted for.

The model

We developed an ecosystem model that was of intermediate complexity as compared with sophisticated ecosystem models aiming at describing processes and structure of forests in detail, and simple index-type evapotranspiration models excluding any process linkages, such as those between transpiration and photosynthesis. We formulated a simple model which predicts evapotranspiration (E) using gross primary production (P) prediction (Fig. 1). Soil water (θ) affects both P and E through simple modifiers, and is described by a frequently used bucket model, which requires minimal input data on soils. θ, on the other hand, also depends on E.

The ecosystem model is called PRELES (PREdict Light-use efficiency, Evapotranspiration and Soil water) and it is intended to be run using standard weather data. The required inputs

are daily mean temperature (T, °C), vapor pressure deficit (D, kPa), precipitation (R, mm), and photosynthetic photon flux density (ϕ, μmol m^{-2} d^{-1}) which can be derived with sufficient accuracy from frequently measured global short-wave radiation. The structural information the model requires is the fraction of absorbed ϕ, which can be estimated from L_A, possibly modified by information about the stand structure (Duursma and Mäkelä 2007).

The PRELES model tracks daily soil-water balance in three storage components: surfacial water (mainly on canopy surfaces due to interception), snow/ice and soil water storages (θ_{surf}, θ_{snow} and θ, respectively). All water storage components are simple bucket models, with no lateral fluxes. Table 1 lists the variables and parameters used in the model.

The dynamic equations of this model can be written as

$$\theta_{surf,k+1} = \theta_{surf,k} + R_k^1 - E_k^{surf} - F_{surf,k} \quad (1)$$

$$\theta_{snow,k+1} = \theta_{snow,k} + R_k^0 - E_k^{snow} - M_k \quad (2)$$

$$\theta_{k+1} = \theta_k + F_{surf,k} + M_k - F_k - E_k^{soil} \quad (3)$$

where all fluxes and storages are daily and expressed in millimetres. The subscript k denotes day, R^1 and R^0 are the rainfall and snowfall (in water equivalents), respectively. We assume that precipitation falls as snow when temperature is below zero. F is the drainage, M is the snowmelt, F_{surf} is the drainage from canopy surfaces to soil, and E consists of components from each of the water storages:

$$E_k = E_k^{surf} + E_k^{snow} + E_k^{soil} \quad (4)$$

We assume that evapotranspiration empties water storages in a sequence from surface, snow, and soil.

Interception is assumed to catch all precipitation up to a surficial water storage maximum, $\theta_{surf,max}$. When this limit is reached, additional precipitation drains to soil water storage θ:

$$F_{surf,k} = \max(0, \theta_{surf} - \theta_{surf,max}) \quad (5)$$

When the effective field capacity of soil, θ_{FC}, is reached, additional water drains away from the system at a rate proportional to current daily soil water content above θ_{FC}.

$$F_k = \frac{\theta_k - \theta_{FC}}{\tau_F} \quad (6)$$

Below θ_{FC} we assumed there is no drainage. τ_F is a delay parameter of drainage, determining the proportional decrease of θ relative to θ_{FC} until it is reached. We estimated τ_F = 3 days using time-series data of soil water measurements.

θ_{snow} accumulates when mean daily temperature $T < 0$ °C and melts when $T > 0$ °C:

$$P_k = \begin{cases} \theta_{snow} m T_k, T_k > 0 \\ 0, T_k \le 0 \end{cases}, \quad (7)$$

where m (°C^{-1} d^{-1}) is a coefficient for temperature dependence of snowmelt rate, following the model presented for snowmelt earlier (Kuusisto 1984).

The modelled water balance can be closed with the above simple rules if E can be estimated. Predicting P is usually easier than predicting E, meaning that P predictions are generally more precise and accurate than those of E. Therefore, our model starts from estimating P with an empirical equation, and P prediction is then used in the empirical E function.

The P submodel was adopted from (Mäkelä *et al.* 2008). It predicts photosynthetic production P_k (P, g C m^{-2} day^{-1}) during day k:

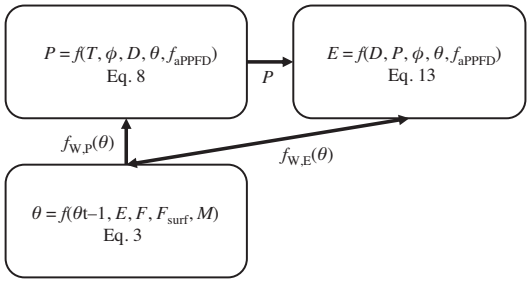

Fig. 1. Dependencies of P, E and θ in the model (*see* Table 1 for explanations of P, E and θ and their units). Equations in the figure (Eqs. 8, 13 and 3) refer to equations in the text. For simplicity, other water storages (θ_{snow} and θ_{surf}) and fluxes between them and the soil water storage, effects of θ_{snow} and θ_{surf} on E, and the other equations used within the referred equations are not shown (*see* text for details).

Table 1. Variables and parameters used in the model.

	Symbol	Unit
Variables (model input or estimated by the model)		
Daily precipitation (water or snow)	R	mm
Drainage	F	mm
Drainage from surfacial water storage to soil (after $\theta_{surf,max}$ is reached)	F_{surf}	mm
Evaporation	E	mm
Evapotranspiration from snow storage	E^{snow}	mm
Evapotranspiration from soil storage	E^{soil}	mm
Evapotranspiration from surficial water storage	E^{surf}	mm
Fraction of absorbed photosynthetic photon flux density	$f_{a\phi}$	–
Gross primary production	P	g C m^{-2}
Leaf area index	L_A	–
Light modifier	f_L	–
Minimum of vapour pressure deficit and soil water modifier	$f_{DW,P}$	–
Modifier for temperature acclimation state, cf. S	f_S	–
Photosynthetic photon flux density	ϕ	mol^{-1} m^{-2}
Rainfall, as rain	R^1	mm
Relative extractable water	W	–
Soil water modifier for evaporation	$f_{W,E}$	–
Snow/ice water content (in water equivalents)	θ_{snow}	mm
Snowfall	R^0	mm
Snowmelt	M	mm
Soil water content	θ	mm
Soil water modifier for gross primary production	$f_{W,P}$	–
State of acclimation to temperature	S	°C
Surfacial water content, e.g. on leaf and soil surfaces (has an upper limit indicated by the subscript 'max')	θ_{surf}	mm
Temperature, daily mean	T	°C
Vapour pressure deficit, daily mean	D	kPA
Vapour pressure deficit modifier	f_D	–
Parameters		
A priori estimate for the state of temperature acclimation	X	°C
Coefficient for temperature dependence of snowmelt rate	m	°C^{-1} d^{-1}
Delay parameter for the response of temperature acclimation state to the changes in ambient temperature	τ	–
Delay parameter of drainage	τ_F	–
Effective field capacity	θ_{FC}	mm
Effective wilting point	θ_{WP}	mm
Evaporation parameter	χ	mm mol^{-1}
Light modifier parameter for saturation with irradiance	γ	mol^{-1} m^{-2}
Parameter adjusting transpiration with D	λ	–
Parameter adjusting transpiration with W	ν	–
Posterior (calibrated) standard deviation for P, E or θ, respectively (used only in model calibration)	σ_P, σ_E, σ_θ	–
Potential light use efficiency	β_P	g C mol^{-1} m^{-2}
Sensitivity parameter of f_D to D	κ	kPa^{-1}
Surfacial water storage maximum	$\theta_{surf,max}$	mm
Threshold above which the state of acclimation increases	X_0	°C
Threshold at which the acclimation modifier reaches its maximum	S_{max}	°C
Threshold for W effect on P in modifier $f_{W,P}$	ρ_P	–
Threshold for W effect on evaporation in modifier $f_{W,E}$	ρ_E	–
Transpiration parameter	α	mm (g C m^{-2} kPa$^{1-\lambda}$)$^{-1}$

$$P_k = \beta_P \phi_k f_{a\phi} \prod_i f_{i,k}, \quad (8)$$

where β_P is the potential light use efficiency (g C mol^{-1} m^{-2}), i.e. the maximum light use efficiency reached in optimal growing conditions and at low light. This parameter has also been found to correlate with canopy mean nitrogen concentration and f_N modifiers have been developed for incorporation of canopy N in the model (Peltoniemi *et al*. 2012), but they were not used in this study. ϕ is the photosynthetic photon flux density (mol m^{-2} day^{-1}) during day k, $f_{a\phi}$ is the fraction of ϕ absorbed by the canopy, and $f_{L,k}$, $f_{S,k}$, and $f_{D,k}$, are the modifiers that account for the suboptimal conditions in light, temperature acclimation, and the minimum of modifiers for vapour pressure deficit ($f_{D,k}$) and soil water ($f_{WP,k}$), respectively, on a day k. All modifiers range from 0 to 1, and thus they scale down the $\beta_{P,k}$.

The *f* modifiers are explained in Mäkelä *et al*. (2008); here we present only a short summary. The light modifer (f_L) describes the saturation of photosynthetic production with high photosynthetic photon flux density ϕ, with $f_L = (\gamma\phi + 1)^{-1}$, where γ is a parameter. With appropriate γ, f_L multiplied by ϕ predicts the saturating effect of high irradiance on P in the form of frequently used rectangular-hyperbola photosynthesis model (Peltoniemi *et al*. 2012). Temperature-related effects are modelled using a modifier for temperature acclimation (f_S).

$$\begin{aligned} &f_{S,k} = \min\left(S_k / S_{max}, 1\right), \text{where} \\ &S_k = \max\left(X_k - X_0, 0\right), \text{where} \\ &X_k = X_{k-1} + \frac{1}{\tau}\left(T_k - X_{k-1}\right), \text{with } X_1 = T_1 \end{aligned} \quad (9)$$

S_k (°C) is the state of acclimation to temperature estimated using a first-order dynamic delay model for a priori estimate for the state of temperature acclimation X_k (°C). It is affected by T_k (°C) on day k, and its value for the previous day (X_{k-1}). τ is a delay parameter for the response of temperature acclimation state to the changes in ambient temperature. X_0 (°C) is a threshold for X_k above which S_k starts to increase f_S. S_{max} (°C) is the threshold value at which the acclimation modifier reaches its maximum, and $S_{max} + X_0$ (°C) is the steady temperature level above which canopy P is not constrained by temperature. This modifier captures the seasonal cycle, as well as the variation in daily temperature, but so that the responses of ambient temperature are delayed (Mäkelä *et al*. 2004, Mäkelä *et al*. 2008).

In the model of Mäkelä *et al*. (2008), water vapour pressure deficit of atmosphere reduced P through an exponential relationship ($f_D = e^{\kappa D}$, where $\kappa < 0$) and a separate modifier were introduced to account for the soil water. Here we modified that representation, assuming that either vapour pressure deficit (D) or soil water effect limits canopy photosynthesis (Landsberg and Waring 1997). Based on this assumption we used a joint water modifier for D and soil water, which uses the estimate of θ of the previous day, and D of the current day to calculate the *f* modifier for the current day:

$$f_{DW,P} = \min(f_D, f_{W,P}), \quad (10)$$

where $f_{W,P}$ is estimated from relative extractable water (W), defined as

$$W = \frac{\theta - \theta_{WP}}{\theta_{FC} - \theta_{WP}}, \quad (11)$$

For the soil water modifier we adopted the widely used threshold model proposed by Granier (Granier 1987), where

$$f_{W,P} = \min(1, W/\rho_P), \quad (12)$$

i.e., $f_{W,P}$ increases linearly with increasing W between 0 and ρ_P that is a threshold of W above which the modifier value is set to 1. Using previous day's estimate for soil water is justifiable because changes in soil water are small during a day when soil water is constraining P.

E was estimated with an empirical model that does not require wind speed, canopy height or net radiation, variables difficult to obtain for broad spatial scales. Coniferous forests have usually rough canopies where the boundary layer conductance is usually much greater than the canopy conductance. This means that transpiration is controlled by canopy conductance (g_c), and much of the variation in transpiration can be expressed by multiplying it by vapour pressure deficit of air (D), i.e. $g_c D$ (Brümmer *et al*. 2012, Jarvis 1976, Whitehead 1998). We considered that daily P is a good predictor of the daily sum of transpiration, i.e,. it contains information

about g_c. Daily average g_c can be estimated from P using a statistical relationship, which accounts for the effects of soil water and D on g_c. We further assumed that radiation drives evaporation on non-stomatal surfaces, i.e. mostly soil and non-stomatal vegetation like mosses (Philip 1957, Schulze *et al*. 1995). The radiation incident on non-green surfaces can be approximated with $(1 - f_{a\phi})\phi$, because photosynthetic photon flux density follows short- and long-wave radiation approximately linearly. This formulation of evapotranspiration requires minimal input data, but allows for a link between P and E and is fairly straightforward and flexible to fit to data.

$$E = \alpha P f_{W,P}^{\nu} D^{1-\lambda} + \chi\left(1 - f_{aPPFD}\right)\phi f_{W,E} \quad (13)$$

where α and χ are the transpiration and evaporation parameters, respectively, which partially determine the fraction of the two water fluxes. In preliminary model fits, P turned out to be an effective predictor of E, but its response was not linear. The λ is the adjustment parameter for the effect of D on transpiration that linearized the response of E to P. The modifier $f_{W,P}$ of the P equation was included in the transpiration part, but raised to power ν because P and E fluxes are not similarly influenced by W. The parameter α is also related to water-use efficiency of vegetation, which is here modified by the terms $f_{W,P}^{\nu}$ and $D^{1-\lambda}$. Their role is to incorporate the different effects of soil water status and D on stomatal opening and therefore on the ratio of E and P. The difference is caused by the increasing CO_2 gradient between the stomatal cavity and air when stomatal aperture is narrow, which influences the CO_2 but not the H_2O uptake rate. Evaporation approximated with the right-hand side of Eq. 13, is also influenced by soil drought, but this relationship is different from that of transpiration, as the resistance of soil to evaporation is created by drying soil layers. It has been reported (Philip 1957) that before the soil is very dry, evaporation can be predicted with negligible error using irradiance, i.e. with an 'isothermal' approach. We thus included a modifier $f_{W,E}$ that reduces evaporation under dry soil; $f_{W,E}$ modifier follows $f_{W,P}$ but has its own threshold parameter ρ_E that was estimated from the data, i.e. $f_{W,E} = \min(1, W/\rho_E)$. Additionally, $f_{W,E} = 1$ when θ_{surf} or θ_{snow} are greater than zero.

Model fits

The calibration of the model for Hyytiälä was conducted jointly for P and E, i.e. the model linkages between P and E, and E and θ were operative during calibration. We simultaneously estimated 13 parameters of the P and E submodels and used measurements of P, E and θ to constrain the model. To estimate the posterior parameter distributions, we summed the log-likelihoods of the P, E, and θ predictions to get a compound log-likelihood, $\ln(\pi)$, for all types of data (Y_j). In addition to these 13 model parameters, we estimated the posterior standard deviations of P, E and θ (σ_P, σ_E, σ_θ) distributions.

We did not calibrate the parameters related to soil. Field capacity, wilting point, and drainage delay above field capacity were estimated separately from the data, and considered input variables to the model. Parameters related to snow melt and accumulation were not calibrated either, as P, E and θ do not properly constrain them. Snow-related parameters were estimated from other data (not shown), as they only have a marginal effect on the questions we investigated.

Similar calibration was made using the Sodankylä data, but we did not use θ measurements to constrain the model.

Calibration algorithm

Assimilation of the P, E and θ data to the model was carried out using an adaptive Metropolis-within-Gibbs algorithm (Rosenthal 2007) which processes batches of each parameter at a time. In each batch, some fixed number of candidates is generated for a parameter from a proposal distribution, which are accepted according to the usual Metropolis-criterion, i.e. each candidate is accepted with a probability $\min(1, \pi_{new}/\pi_{old})$. After each batch, the algorithm adapts the proposal distribution of that parameter by a small increment, with the aim of finding better mixing and convergence for this chain. The algorithm then moves to the next parameter, continuing until the maximum chain length is reached.

A posterior distribution of the parameter vector $\boldsymbol{X}$ (*see* Fig. 2 for the calibrated parameters) of the model conditional on the data vector

$\boldsymbol{Y}$ (measurements of E, P and θ), $\pi(\boldsymbol{X}|\boldsymbol{Y})$, was obtained with Bayesian inversion, and by applying the above adaptive Markov Chain Monte Carlo (MCMC) algorithm. We assumed that all measurements of the vector $\boldsymbol{Y}$ were normally distributed and independent, and that parameters had uniform prior distributions. The posterior probability of the model parameters equals the likelihood of the data $\pi(\boldsymbol{Y}|\boldsymbol{X})$. This gives natural logarithms of likelihood of each of the data series j (P, E and θ) in the form:

$$\begin{aligned}\ln L_j &= \ln \pi\left(\boldsymbol{Y}_j \middle| \boldsymbol{X}\right) = \ln\left(\boldsymbol{X} \middle| \boldsymbol{Y}_j\right) \\ &= -0.5 \ln 2\pi - \ln \sigma_j \\ &- 0.5 \sum_i^n \frac{\left[Y_{j,i} - \hat{Y}_{j,i}\left(\boldsymbol{X}\right)\right]^2}{\sigma_j^2}\end{aligned}. \quad (14)$$

The sum of $\ln L_j$ for the data series $j \in \{P, E,$ and $\theta\}$ was used in the Metropolis acceptance criterion. Outside the prior range, the likelihood was set to a very large negative value to express zero probability for π.

Convergence of the MCMC chains was examined by running several chains in parallel, and by examining each chain visually. The chains started from different random initial values. Additionally we performed a convergence test of Heidelberg and Welch (1983) to test convergence quantitatively. In all cases, the parameter chains converged quickly to provide samples from the same posterior by 9000 samples. We then discarded 10 000 samples from each chain as a burn-in period, after which 20 000 samples were used for further analyses.

Model evaluation

We present the mean responses of the model by using the calculated 95% confidence limits of the model-simulated daily predictions of P, E, and θ. In order to calculate these limits, we performed 400 model runs using 400 parameter samples from the posterior distributions (every 50th sample from converged part of the chain). The lower and upper confidence limits for each day were calculated as the 2.5 and 97.5 percentiles of daily model predictions. Between them 95% of responses of the model are located; 95% confidence limits of the predictions were created in a similar fashion. In order to estimate these confidence limits, we generated samples of P, E and θ from their probability distributions (normal distributions). The above-mentioned model predictions of P, E and θ in 400 model runs and associated σ_P, σ_E, and σ_θ from the posterior distributions were used as the means and standard deviations of the distributions, respectively.

Model fits were evaluated both with the calibration data (1998–2009) and with additional three years of the data from Hyytiälä (2010–2012, gap-filled observations). The model fit for the Hyytiälä data was also tested with the Sodankylä data (2003–2008), and its predictions were compared with the Sodankylä model fit.

We assessed the model fits in terms of coefficient of determination (r^2) and by calculating the average deviation of the model predictions ($\hat{y}_k$) from the measurements (y_k), using the formula of the arithmetic mean (*see* e.g. Smith *et al*. (1997) for various metrics used in model evaluation), henceforth called bias, i.e. bias = $\sum_k^n \left(y_k - \hat{y}_k\right)/n$. It was estimated from the daily data for n days for which the data were not missing, and from predictions made with the parameter set with the highest likelihood. For the years 2010–2012, the gap-filled data were used in the evaluation.

We also evaluated the calibrated model by examining its behaviour when applied to a hypothetical stand (more or less L_A) and soil structures (higher or lower soil water storage), using Hyytiälä 2006 input data.

Sensitivity analyses

Sensitivity of the model predictions to its parameters [$S_y(x) = \partial y/\partial x$] is partially dependent on the model state (soil water content) and weather input, so we simulated the effects of small changes (1%) of model parameters x, on responses y (P, E, θ, f_W) for all the years and days of the study. Sensitivities are presented for two representative years, which were the wet year 1998 and the dry year 2006. Six most sensitive parameters were selected based on their average sensitivities during these years, and their daily courses in these years were then plotted to show the dependencies of sensitivities on model state and season.

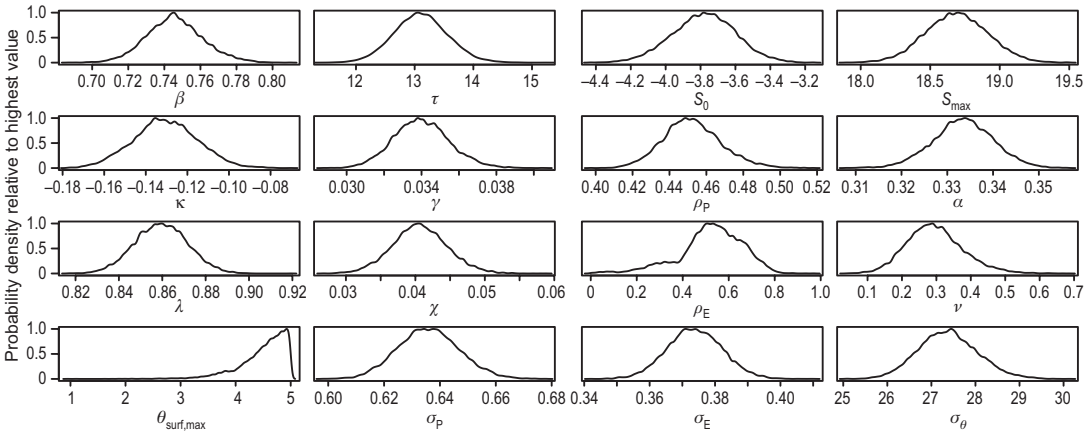

Fig. 2. Probability densities of model parameters in Hyytiälä calibration.

Results

All parameter chains converged towards their final distributions with plausible mean values, most of them showing a close-to-Gaussian distribution (Fig. 2, *see* also Table 2). Highest parameter correlations were between *P* model parameters related to potential light-use efficiency (β_P) and light modifier parameter for saturation with irradiance (γ), and γ and the parameter responsible for the sensitivity of f_D to *D* (κ); as well as between *E* model parameters related to transpiration (α) and its adjustment with *D* (λ), and λ and evaporation coefficient (χ). These high correlations between parameters indicate that they partially compensated the effects of each other, and that special care should be taken when these model parameters are adjusted to new locations (Fig. 3). Predictions of *P* and *E* followed closely those in the calibration dataset (Fig. 4), and the posterior standard deviations of those predictions (σ_P and σ_E), were 5.5% and 8.6% of the maximum measured *P* and *E*, respectively.

Fit statistics for the model fitted to the data

Table 2. Model parameter estimates for Hyytiälä and Sodankylä calibrations. L_{max} is the parameter set with the highest likelihood, and SD is the standard deviation of parameter's posterior distribution.

Parameter	Hyytiälä			Sodankylä		
	L_{max}	mean	SD	L_{max}	mean	SD
β_P	0.748	0.746	0.0153	0.826	0.826	0.049
τ	12.7	13.1	0.457	13	13	0.696
S_0	–3.57	–3.77	0.185	–2.73	–2.72	0.245
S_{max}	18.5	18.7	0.234	19.5	19.5	0.662
κ	–0.137	–0.131	0.0154	–0.13	–0.132	0.0298
γ	0.0339	0.034	0.00145	0.0485	0.0482	0.00435
ρ_P	0.449	0.452	0.0159	0.0733	0.177	0.106
α	0.333	0.334	0.0069	0.284	0.284	0.00791
λ	0.857	0.859	0.0123	1.07	1.07	0.0183
χ	0.0418	0.041	0.00403	0.0292	0.0286	0.00203
ρ_E	0.474	0.524	0.138	0.999	0.987	0.0127
η	0.278	0.295	0.0829	–	–	–
$\theta_{surf,max}$	4.82	4.5	0.438	1.66	1.05	0.878
P	0.641	0.636	0.0111	0.661	0.666	0.0128
E	0.377	0.374	0.00849	0.34	0.34	0.00655
θ	27.1	27.4	0.684	–	–	

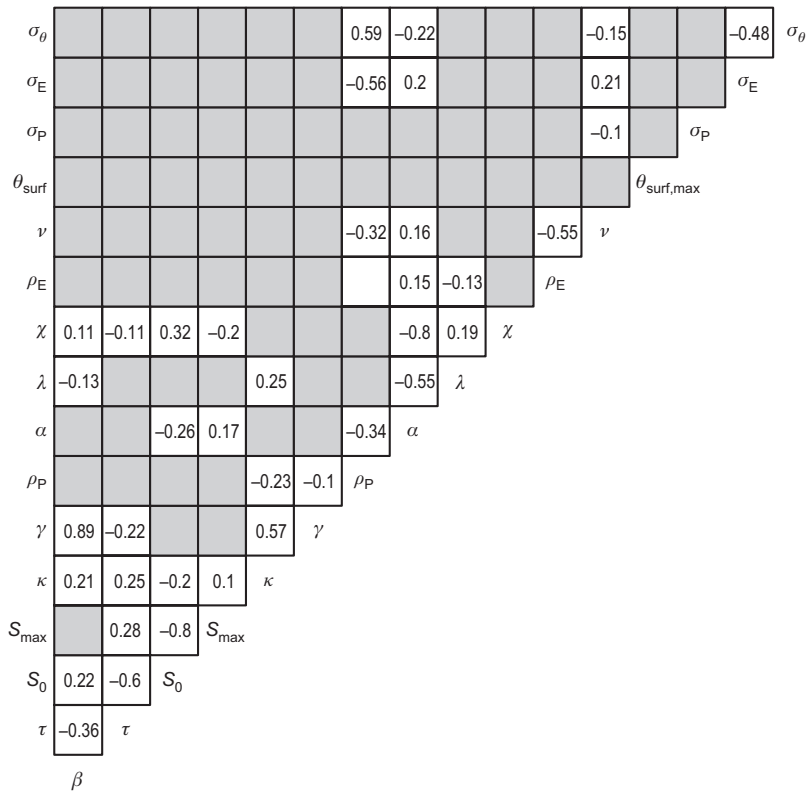

Fig. 3. Correlations between model parameters. Grey indicates no correlation.

of all the years differed to some extent between the years (solid lines in Fig. 5), but the goodness of fit of P predictions was consistently high (fit years: $r^2 = 0.96$, bias = 0.03 g C m^{-2}, $n = 1755$, test years: $r^2 = 0.96$, bias = 0.05 g C m^{-2}, $n = 641$). In contrast, the goodness of fit of E was weaker, and the model tended to overestimate E, especially early in the season and for moist conditions (fit years: $r^2 = 0.89$, bias = –0.08 mm, $n = 1755$, test years $r^2 = 0.91$, bias = –0.01 mm, $n = 1095$). The goodness of fit for θ was the weakest among these variables (fit years: $r^2 = 0.79$, bias = –0.21 mm, $n = 1415$, test years $r^2 = 0.59$, bias = –0.34 mm, $n = 636$), but the model replicated the trends in θ (Fig. 6).

According to the sensitivity analyses, γ had the most pronounced effects on all of the investigated responses (P, E, and θ, and f_W), and its effect was amplified in the dry year (Fig. 7). Parameters related to soil water storage capacity (θ_{FC} and θ_{WP}) were among the most sensitive variables, but played a small role in the wet year. The six most sensitive parameters had a clear seasonal pattern, often with more notable sensitivity in the dry year (Fig. 8). For example, the general tendency of P to decrease when γ increased was reversed in dry conditions, because the increases of γ actually saved soil water, which increased P more than γ reduced P through the f_L equation. Similarly, the signs of sensitivities to potential light use efficiency (β_P) and to the evapotranspiration model parameters α and χ were reversed under drought.

Predictions of P for Sodankylä using the model fitted with the Hyytiälä data correlated well with the measurements from the Sodankylä eddy-covariance site ($r^2 = 0.87$, $n = 2192$), but were somewhat overestimated (average bias on 2003–2008 was –0.24 g C m^{-2}). The model fitted using the Sodankylä data had $r^2 = 0.88$ and bias = 0.01 g C m^{-2} ($n = 2192$). The Sodankylä prediction with Hyytiälä calibration was particularly good in 2006 ($r^2 = 0.93$, bias = –0.19 g C m^{-2}, $n = 2192$), when it also predicted that the reduction in measured P in August–September was due to low soil water, an explanation

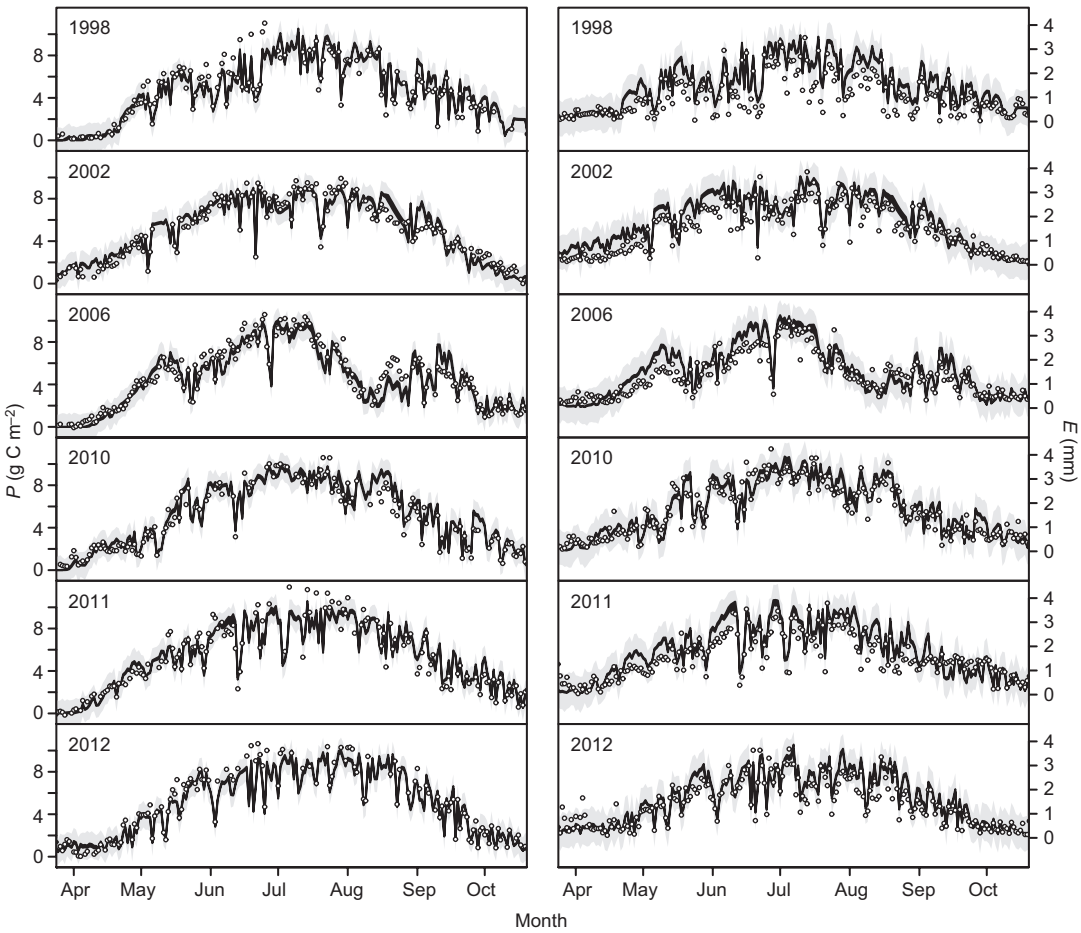

Fig. 4. Predictions of *P* and *E* in three calibration years and three test years (2010–2012) in Hyytiälä. Circles are measurements. Black line of variable width is the confidence interval of the mean model response, while grey area depicts the confidence interval of model predictions.

that did not emerge from the Sodankylä calibration (r^2 = 0.91, bias = 0.02 g C m^{-2}, n = 2192) (Fig. 9). The decreasing soil water was driven by modelled *E* (with Hyytiälä parameters) that was somewhat higher than measured in Sodankylä (HY calibration for *E*: r^2 = 0.75, n = 2192, bias = –0.09 mm i.e. 15%–18%, depending on year; SD calibration: r^2 = 0.76, n = 2192, bias = 0.24 mm).

In order to understand how stand $f_{a\phi}$ and soil water storage capacity affect annual total *P* and *E*, we varied these inputs and investigated the model behaviour (with the highest likelihood calibration) in hypothetical cases using the Hyytiälä 2006 weather data. First, we increased and decreased the water holding capacity of the soil by 70% in order to represent hypothetical responses of a wet and dry site. The reductions severely limited annual *P*, while the increases had a lesser positive effect. Second, we tested the effect of sparser and denser canopy on the predictions. Cumulative *P* increased nearly in proportion with increasing canopy cover (expressed as $f_{a\phi}$) but cumulative *E* did not increase similarly because evaporation nearly compensated transpiration (Fig. 10). However, off-season evapotranspiration was predicted to be higher at the sparse site than at the dense site, while the opposite occurred during the growing season. The model also predicted the snow melt to occur four days earlier and the maximum snow water equivalent to be higher at the sparse site than at the dense site, because decreasing $f_{a\phi}$ means a

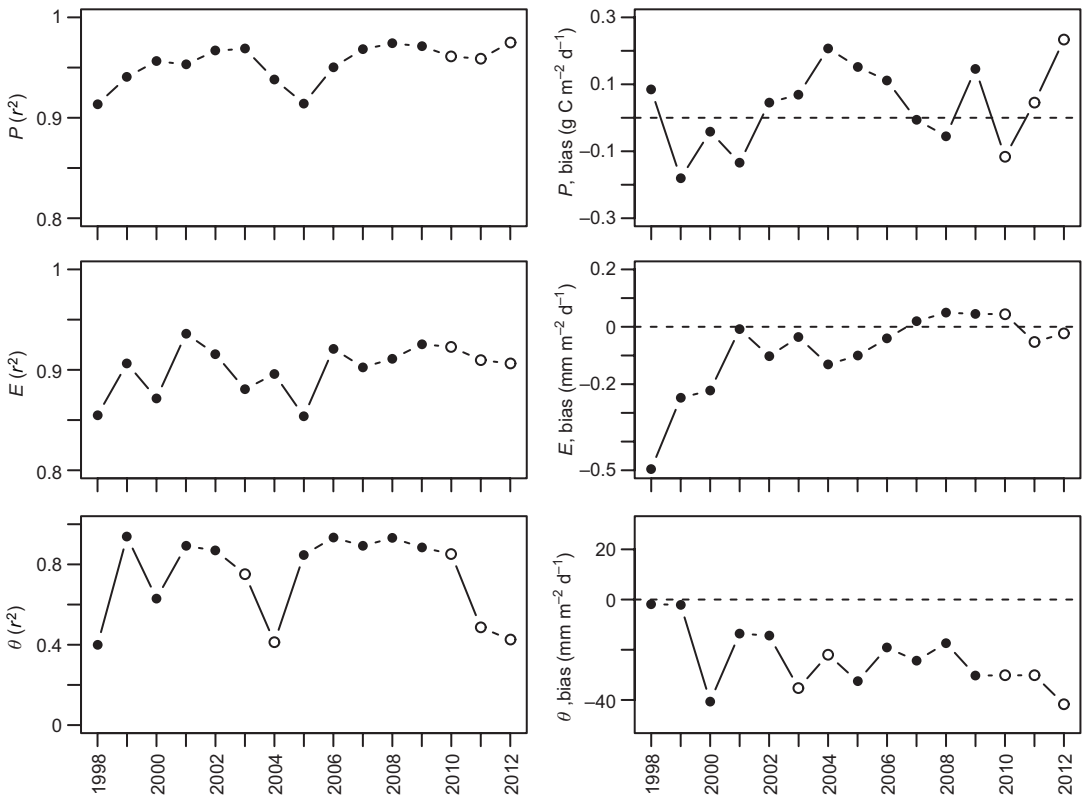

Fig. 5. Coefficients of determination and bias of the fits of the model. Circles denote test data, i.e., the data and years omitted from calibration. Number of observations was different for different years, $n = 75–233$ (P), $n = 75–207$ (E), $n = 74–212$ (θ, for accepted years).

higher evaporation fraction in the model which also acts during the winter.

Discussion

Here, we formulated a simplified model of ecosystem water and carbon exchange based on the interaction of photosynthesis, evapotranspiration and soil water content. The key motivation for the study was to develop an ecologically-based model that would be widely applicable due to the feasibility of model inputs.

Model calibrations were consistent and provided good fits for both Hyytiälä and Sodankylä, especially for P and for most years also for E, while soil water content was least accurately reproduced (Fig. 5). For evaluating the transferability of the model, we tested the model using three additional years of measurements in Hyytiälä and five years of data from the Sodankylä eddy-covariance site. The predicted fluxes for the test years in Hyytiälä were as good as in the calibration dataset, but again, measurements of soil water showed higher deviation. This may be partially attributed to the renovation of the soil water measurement instruments in the summer of 2011 when new TDR sensors similar to the original ones were installed in the original positions in the soil profiles.

The parameter sets obtained for the two sites were very similar, except for ρ_P, ρ_E and $\theta_{surf,max}$, the two former parameters related to soil water content for which there were no measurements in Sodankylä. The Hyytiälä values for ρ_P and ρ_E were consistent with previous empirical and theoretical evaluations of the threshold water contents for photosynthesis and evapotranspiration, while the Sodankylä values were not (Granier *et al*. 2007). The Hyytiälä parameter

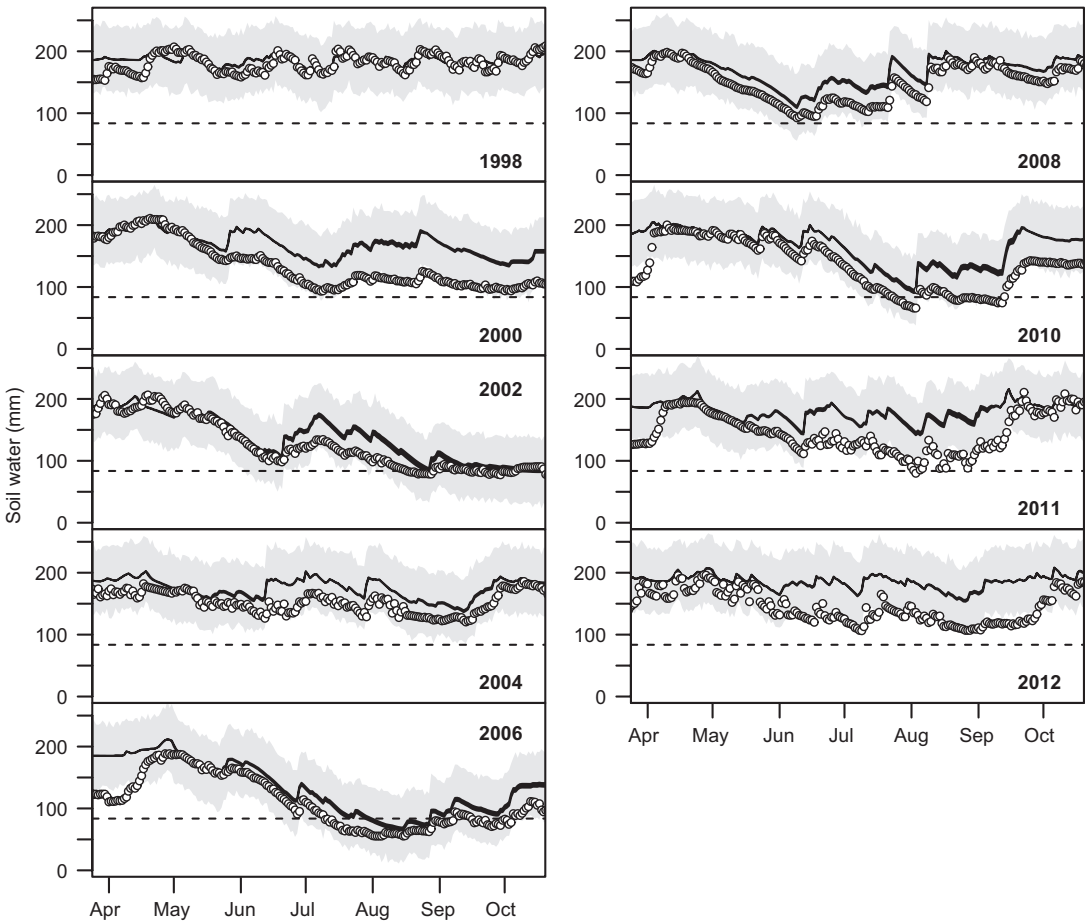

Fig. 6. Predictions of soil water content for even years in the calibration data set in Hyytiälä (1998–2009) and for three additional years for model evaluation (2010–2012). Measurements are shown as circles. Black lines of variable width indicate confidence intervals of the mean response, while the grey area represents the 95% confidence intervals of predictions. New soil water instruments were installed in summer 2011; these new estimates may not fully comply with earlier measurements.

set correlated nearly as well with measured P and E, and so did the Sodankylä parameters, though with some overestimation of E. It is interesting to note that the Hyytiälä calibration performed better in Sodankylä for the drought period of 2006 suggesting that the information based on the Hyytiälä site was useful for predictions under drought conditions in Sodankylä. In the Sodankylä calibrations, there seemed to be little data to associate drought with P, and the fitted P reduction threshold (ρ_p) became much lower than in Hyytiälä.

Previous studies also found that physiological parameters are transferable between sites. Similar seasonal-temperature responses of photosynthesis have been shown for Hyytiälä and a sub-arctic pine site in Värriö, Finland (Kolari *et al*. 2007). Mäkelä *et al*. (2008) showed for seven European sites that most parameters of their light-use-efficiency-based model were transferable between sites, although site-specific calibration provided best results overall. Duursma *et al*. (2009) concluded that the main drivers of differences in model predictions of canopy photosynthesis between sites were climate and leaf area, while differences in physiological parameters played a minor role.

Based on the comparison between Sodankylä and Hyytiälä, information on soil water appears crucial for model calibration, but even when data

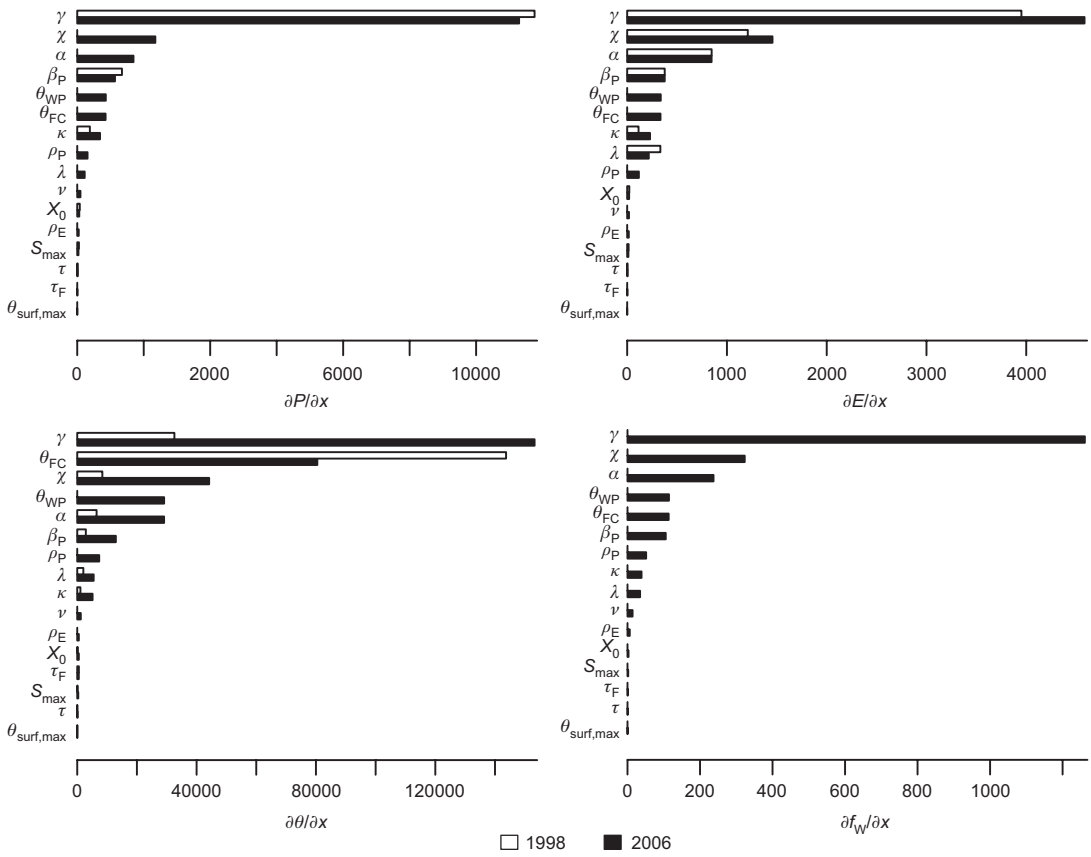

Fig. 7. Model parameter sensitivities in a wet (1998) and dry (2006) year for P, E, θ, and $f_{W,P}$.

are available soil water is the component that shows the worst fit with the data. The results could probably have been improved, if we had allowed the parameters related to soil water-holding capacity to vary in the MCMC analysis, however, we decided to fix those parameters because they had been evaluated in direct measurements. As a rule, the best fit simulations overestimated soil water content. Because the effect of water availability on P and E is modelled as a threshold process, the impact of this on model predictions will be to underestimate the occurrence of drought, but during non-drought conditions there would be no bias caused by soil water.

Part of the problems with soil water prediction could stem from the uncertainty of measured water balance components. Model predicted higher E than the average measured in Hyytiälä (bias = –0.08 mm d^{-1}, i.e. 30 mm a^{-1}). To evaluate whether such overestimation is plausible, we compared our evapotranspiration predictions with potential evapotranspiration (PET) calculated using a method devised by FAO and based on the Penman-Monteith equation and interpolation of long-term weather station data (Grieser *et al*. 2006). This gave a PET value of 543 mm for Hyytiälä and 320 mm for Sodankylä, while our predictions of actual evapotranspiration were 331–394 mm for Hyytiälä and 206–233 mm for Sodankylä in 1998–2007. Even when we increased the soil water-holding capacity in our sensitivity analysis, actual evapotranspiration remained below 400 mm in Hyytiälä, which is only 74% of the PET provided by the FAO method. Flux measurements indicated that annual E is 246–368 mm for Hyytiälä and 208–253 mm for Sodankylä in 2003–2008. In

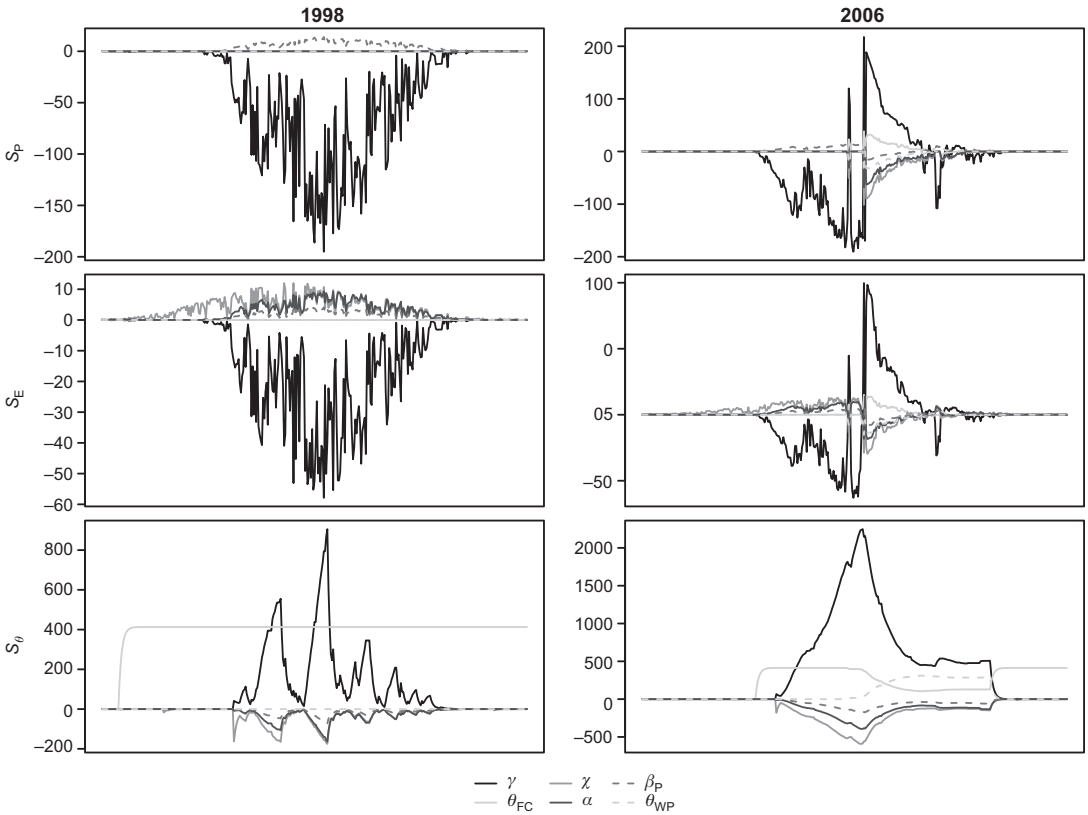

Fig. 8. The annual course of selected parameter sensitivities and inputs in the wet (1998) and dry (2006) years. The sensitivity of model parameters is partially dependent on environmental variables and states of the modelled water storages, i.e., water contents. High sensitivity values imply that the model prediction is sensitive to the variable indicated on the *y*-axis. Different sensitivities of *P* during 1998 are difficult to identify because they overlap with the zero line.

an analysis of the full water budget for Hyytiälä, Ilvesniemi *et al*. (2010) concluded that for the closure of the water balance, the measurements of either evapotranspiration (measured as latent heat flux) or drainage had to be underestimated by up to 20%. We, therefore, conclude that the model benefitted from the calibration with the soil-water measurements from Hyytiälä, which resulted in plausible evapotranspiration estimates (at least for the entire year), even though it seemed to overestimate *E* in comparison with the data.

The sensitivity analyses (Fig. 7) showed that the prediction of photosynthesis was highly sensitive to β_P and γ which were also found to be correlated (Fig. 3). This is understandable as β_P is a multiplier in the photosynthesis expression (Eq. 8), while γ determines the degree of nonlinearity of the response of photosynthesis to photosynthetic photon flux density. Because evapotranspiration increases with increasing photosynthesis (Eq. 13), *E* is also sensitive to the same parameters as *P*. While extending the model use to other species than Scots pine, e.g. by using canopy N-concentration–β_P relationship developed earlier (Peltoniemi *et al*. 2012) one should note that the reported N relationship increase in *E*.

Evapotranspiration was also sensitive to α and χ which are the linear multipliers of the transpiration and evaporation components of *E*, respectively. These parameters were also important for *P* during the dry year, due to the connection of *P* and *E* through θ (Figs. 7 and 8). This reflects the property of the model that larger evapotranspiration dries up the soil faster, which subsequently reduces photosynthesis through decreased stomatal conductance quantified by

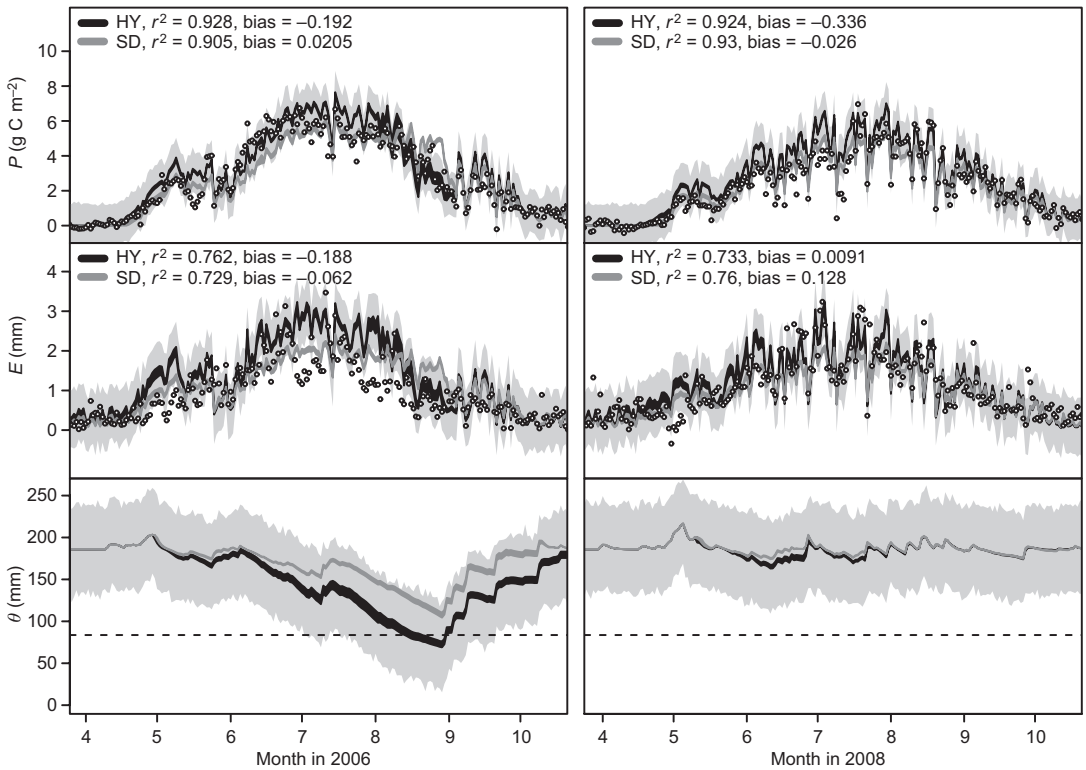

Fig. 9. Model predictions for the Sodankylä site. Predictions of two calibrations are shown. HY = the model calibrated to Hyytiälä data (black lines of variable width show confidence intervals of the mean response, and light-grey confidence intervals of prediction). SD = the model calibrated to the Sodankylä data (dark-grey lines of variable width are confidence intervals of mean response). In the top four panels, circles indicate data measured in Sodankylä. In the two bottom panels, we compare soil water predictions made with HY and SD calibrations. Soil parameters were the same as in Hyytiälä in both cases. Two years are shown: in 2006 HY calibration predicted *P* slightly better, whereas in other years SD calibration (2008 as an example) was better.

$f_{W,P}$ and $f_{W,E}$. Again, had we applied the model to species with higher β_p, we would have seen quicker development of drought. Associated with this, κ increased its sensitivity on all predicted variables on the dry year. As κ was also fairly important for the development of drought, further work is required to quantify its variation and find out how it co-varies with β_p and γ across species.

Clearly, more work is needed to extend the calibration data set to more sites with a wider range of L_A and other characteristics. For this, the α and χ are crucial, because they separate the transpiration under stomatal control from evaporation from other surfaces. As these were among the most sensitive and correlated model parameters, and had fairly broad probability density distributions, acquiring more data on their values is important. Here, a lower estimate of χ was obtained for Sodankylä (0.029) than for Hyytiälä (0.042–0.051) (Table 2). While this may simply reflect the inability of the data to constrain χ adequately, one should not dismiss the possibility that χ actually depends on site-specific characteristics. The higher estimate of χ for Hyytiälä could be explained by the fact that Hyytiälä's field layer more closely resembles a wet surface, due to denser canopy and relatively moist ground vegetation and soil. Describing such differences would call for improving the soil-water model to incorporate the top soil as a separate layer, with a faster response to atmospheric drivers than deeper soil layers (Linkosalo *et al*. 2013). In any case, data from contrasting sites is required for the calibration and further improvement of the model.

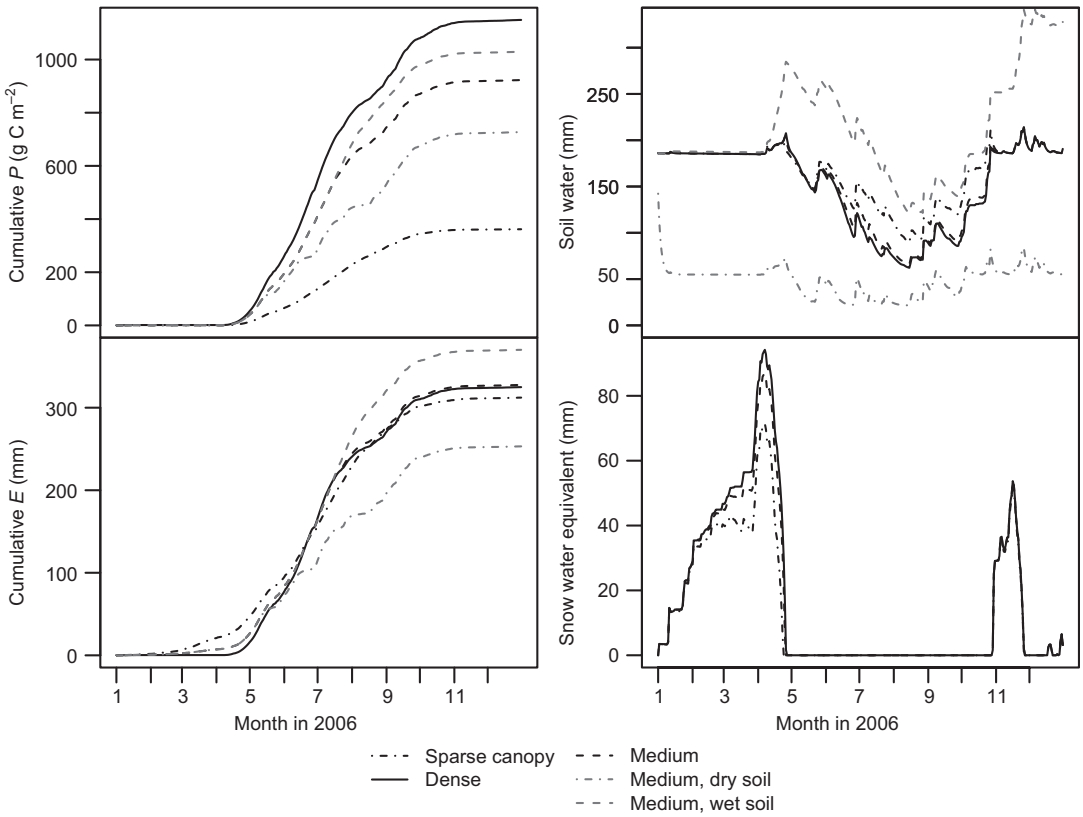

Fig. 10. Predictions of the model for cumulative *P* and *E*, and for θ and snow water equivalent at hypothetical sites using Hyytiälä weather data. The initial reduction of θ in the medium-canopy-dry-soil simulation is due to soil water initialization with a value exceeding θ_{FC} of that site. The average annual f_W were 0.98, 0.89, and 0.92 under sparse, dense and medium canopies, respectively, assuming Hyytiälä soil, and 0.85 and 0.95 under medium canopy with dry and wet soil, respectively.

We consider that simple modelling approaches can be useful for two main reasons. Firstly, determining the capacity of different kinds of soils to store and release water is a global problem, and good quality data are available for few intensively-measured sites only. Secondly, there seems to be some similarity in how and when plants experience drought. A recent study showed that there exists similarity in the physiological vulnerability of trees. Vulnerability is independent of mean annual rainfall at the growth site (Choat *et al*. 2012), suggesting that trees have acclimatized to their current environment by developing very similar safety margins against drought. Another recent study in Finland found that a similar fractions of Scots pine (19%) and Norway spruce (24%) dominated sites suffered from drought damage in an extremely dry year 2006 (Muukkonen *et al*. 2015), supporting the idea that physiological and structural features of trees at different type of sites may have acclimated and adapted so as to reach nearly equal sensitivity to climatic drought. Sites dominated by deciduous species, yet often moist, seemed more vulnerable to drought damages (39%), which could stem from the less conservative water use strategies of deciduous species (Choat *et al*. 2012). These notions imply that increasing the detail of soil water modelling may not increase the reliability of *P* predictions, rather a more holistic approach based on the assumption of acclimation of species under changing environmental could be better (e.g. McMurtrie *et al*. 2008). We found calibration of multiple ecosystem model parameters against several constraining variables par-

ticularly useful for a model, which is partially empirical in nature and intended for prognosis purposes. We expect further work and testing of the model to provide more insights into the possibilities of predicting ecosystem responses to weather and climate.

Acknowledgements: We thank Tapio Linkosalo, Remko Duursma, Teemu Hölttä, Juha Heikkinen for discussions on model development and calibration. We thank the Academy of Finland (grant no. 128236) and European Union Life+ programme (project no. LIFE09 ENV/FI/000571) for the funding this work.

References

Aurela M., Lohila A., Tuovinen J., Hatakka J., Riutta T. & Laurila T. 2009. Carbon dioxide exchange on a northern boreal fen. *Boreal Environment Research* 14: 699–710.

Aurela M. 2005. Carbon dioxide exchange in subarctic ecosystems measured by a micrometeorological technique. *Finnish Meteorological Institute Contributions* 51: 1–132.

Baldocchi D.D. 2014. Measuring fluxes of trace gases and energy between ecosystems and the atmosphere — the state and future of the eddy covariance method. *Global Change Biology* 20: 3600–3509.

Bartlett P.A., Harry McCaughey J., Lafleur P.M. & Verseghy D.L. 2003. Modelling evapotranspiration at three boreal forest stands using the CLASS: tests of parameterizations for canopy conductance and soil evaporation. *International Journal of Climatology* 23: 427–451.

Bergh J., Freeman M., Sigurdsson B., Kellomäki S., Laitinen, K., Niinistö S., Peltola H. & Linder S. 2003. Modelling the short-term effects of climate change on the productivity of selected tree species in Nordic countries. *Forest Ecology and Management* 183: 327–340.

Brümmer C., Black T.A., Jassal R.S., Grant N.J., Spittlehouse D.L., Chen B., Nesic Z., Amiro B.D., Arain M.A. & Barr A.G. 2012. How climate and vegetation type influence evapotranspiration and water use efficiency in Canadian forest, peatland and grassland ecosystems. *Agricultural and Forest Meteorology* 153: 14–30.

Choat B., Jansen S., Brodribb T.J., Cochard H., Delzon S., Bhaskar R., Bucci S.J., Field T.S., Gleason S.M., Hacke U.G., Jacobsen A.L., Lens F., Magerali H., Martínez-Vilalta J., Mayr S., Mencuccini M., Mitchell P.J., Nardini A., Pittermann J., Pratt R.B., Sperry J.S., Westoby M., Wright I.J. & Zanne A.E. 2012. Global convergence in the vulnerability of forests to drought. *Nature* 491: 752–755.

Duursma R. & Mäkelä A. 2007. Summary models for light interception and light-use efficiency of non-homogeneous canopies. *Tree Physiology* 27: 859–870.

Duursma R., Kolari P., Peramaki M., Pulkkinen M., Makela A., Nikinmaa E., Hari P., Aurela M., Berbigier P., Bernhofer Ch., Grünwald T., Loustaum D., Mölder M., Verbeeck H. & Vesala T. 2009. Contributions of climate, leaf area index and leaf physiology to variation in gross primary production of six coniferous forests across Europe: A model-based analysis. *Tree Physiology* 29: 621–39.

Farquhar G.D., Caemmerer S. & Berry J. 1980. A biochemical model of photosynthetic CO_2 assimilation in leaves of C3 species. *Planta* 149: 78–90.

Granier A. 1987. Evaluation of transpiration in a Douglas-fir stand by means of sap flow measurements. *Tree Physiology* 3: 309–320.

Granier A., Reichstein M., Bréda N., Janssens I. A., Falge E., Ciais P., Grünwald T., Aubinet M., Berbigier P., Bernhofer C., Buchmann N., Facini O., Grassi G., Heinesch B., Ilvesniemi H., Keronen P., Knohl A., Köstner B., Lagergren F., Lindroth A., Longdoz B., Loustau D., Mateus J., Montagnani L., Nys C., Moors E., Papale D., Peiffer M., Pilegaard K., Pita G., Pumpanen J., Rambal S., Rebmann C., Rodrigues A., Seufert G., Tenhunen J., Vesala T. & Wang Q. 2007. Evidence for soil water control on carbon and water dynamics in European forests during the extremely dry year: 2003. *Agricultural and Forest Meteorology* 143: 123–145.

Grieser J., Gommes R. & Bernardi M. 2006. New LocClim — the local climate estimator of FAO. *Geophysical Research Abstracts* 8, 08305, SRef-ID: 1607-7962/gra/EGU06-A-08305.

Hari, P. & Kulmala, M. 2005: Station for Measuring Ecosystem–Atmosphere Relations (SMEAR II). *Boreal Environment Research* 10: 315–322.

Ilvesniemi H., Levula J., Ojansuu R., Kolari P., Kulmala L., Pumpanen J., Launiainen S., Vesala T. & Nikinmaa E. 2009. Long-term measurements of the carbon balance of a boreal Scots pine dominated forest ecosystem. *Boreal Environment Research* 14: 731–753.

Ilvesniemi H., Pumpanen J., Duursma R., Hari P., Keronen P., Kolari P., Kulmala M., Mammarella I., Nikinmaa E. & Rannik Ü. 2010. Water balance of a boreal Scots pine forest. *Boreal Environment Research* 15: 375–396.

IPCC 2007: *Climate change 2007: synthesis report*. Contribution of Working Groups I, II and III to the Fourth Assessment Report of the Intergovernmental Panel on Climate Change, IPCC, Geneva, Switzerland.

Jansson P. & Moon D.S. 2001. A coupled model of water, heat and mass transfer using object orientation to improve flexibility and functionality. *Environmental Modelling & Software* 16: 37–46.

Jarvis P.G. 1976. The interpretation of the variations in leaf water potential and stomatal conductance found in canopies in the field. *Philosophical Transactions of the Royal Society London B* 273: 593–610.

Jylhä K., Ruosteenoja K., Räisänen J., Venäläinen A., Tuomenvirta H., Ruokolainen L., Saku S. & Seitola S. 2009. Arvioita Suomen muuttuvasta ilmastosta sopeutumis-tutkimuksia varten. ACCLIM-hankkeen raportti 2009 [The changing climate in Finland: estimates for adaptation studies. ACCLIM project report 2009]. *Ilmatieteen laitos, Raportteja* 2009:4: 1–102. [In Finnish with abstract, extended abstract and captions to figures and tables in English].

Kelliher F.M., Leuning R. & Schulze E.D. 1993. Evaporation and canopy characteristics of coniferous forests and grasslands. *Oecologia* 95: 153–163.

Kolari P., Lappalainen H.K., Hänninen H. & Hari P. 2007. Relationship between temperature and the seasonal course of photosynthesis in Scots pine at northern timberline and in southern boreal zone. *Tellus* 59B: 542–552.

Kolari P., Pumpanen J., Rannik Ü., Ilvesniemi H., Hari P. & Berninger F. 2004. Carbon balance of different aged Scots pine forests in Southern Finland. *Global Change Biology* 10: 1106–1119.

Kolari P., Kulmala L., Pumpanen J., Launiainen S., Ilvesniemi H., Hari P. & Nikinmaa E. 2009. CO_2 exchange and component CO_2 fluxes of a boreal Scots pine forest. *Boreal Environment Research* 14: 761–783.

Kuusisto E. 1984. Snow accumulation and snowmelt in Finland. *Publications of Water Research Institute* 55: 1–149.

Landsberg J.J. & Waring R.H. 1997. A generalised model of forest productivity using simplified concepts of radiation-use efficiency, carbon balance and partitioning. *Forest Ecology and Management* 95: 209–228.

Lauren A., Finer L., Koivusalo H., Kokkonen T., Karvonen T., Kellomäki S., Mannerkoski H. & Ahtiainen M. 2005. Water and nitrogen processes along a typical water flowpath and streamwater exports from a forested catchment and changes after clear-cutting: a modelling study. *Hydrology and Earth System Sciences* 9: 657–674.

Leuning R. 1995. A critical appraisal of a combined stomatal-photosynthesis model for C3 plants. *Plant, Cell & Environment* 18: 339–355.

Linkosalo T., Kolari P. & Pumpanen J. 2013. New decomposition rate functions based on volumetric soil water content for the ROMUL soil organic matter dynamics model. *Ecological Modelling* 263: 109–118.

Mäkelä A., Hari P., Berninger F., Hänninen H. & Nikinmaa E. 2004. Acclimation of photosynthetic capacity in Scots pine to the annual cycle of temperature. *Tree Physiology* 24: 369–376.

Mäkelä A., Pulkkinen M., Kolari P., Lagergren F., Berbigier P., Lindroth A., Loustau D., Nikinmaa E., Vesala T. & Hari P. 2008. Developing an empirical model of stand GPP with the LUE approach: analysis of eddy covariance data at five contrasting conifer sites in Europe. *Global Change Biology* 14: 92–108.

Mammarella I., Launiainen S., Grönholm T., Keronen P., Pumpanen J., Rannik Ü. & Vesala T. 2009. Relative humidity effect on the high-frequency attenuation of water vapor flux measured by a closed-path eddy covariance system. *Journal of Atmospheric and Oceanic Technology* 26: 1856–1866.

McMurtrie R.E., Norby R.J., Medlyn B.E., Dewar R.C., Pepper D.A., Reich P.B. & Barton C.V.M. 2008. Why is plant-growth response to elevated CO_2 amplified when water is limiting, but reduced when nitrogen is limiting? A growth-optimization hypothesis. *Functional Plant Biology* 35: 521–534.

Moffat A.M., Papale D., Reichstein M., Hollinger D.Y., Richardson A.D., Barr A.G., Beckstein C., Braswell B.H., Churkina G., Desai A.R., Falge E., Gove J. H., Heimann M., Hui D., Jarvis A.J., Kattge J., Noormets A. & Stauch V.J. 2007. Comprehensive comparison of gap-filling techniques for eddy covariance net carbon fluxes. *Agricultural and Forest Meteorology* 147: 209–232.

Monteith J.L. 1965. Evaporation and environment. *Symposia of the Society for Experimental Biology* 19: 204–234.

Muukkonen P., Nevalainen S., Lindgren M. & Peltoniemi M. 2015. Spatial occurrence of drought-associated damages in Finnish boreal forests: results from forest condition monitoring and GIS analysis. *Boreal Environment Research* 20: 172–180.

Papale D., Reichstein M., Aubinet M., Canfora E., Bernhofer C., Kutsch W., Longdoz B., Rambal S., Valentini R., Vesala T. & Yakir D. 2006. Towards a standardized processing of net ecosystem exchange measured with eddy covariance technique: algorithms and uncertainty estimation. *Biogeosciences* 3: 571–583.

Peltoniemi M., Pulkkinen M., Kolari P., Duursma R.A., Montagnani L., Wharton S., Lagergren F., Takagi K., Verbeeck H., Christensen T., Vesala, T., Falk, M., Loustau, D. & Mäkelä A. 2012. Does canopy mean nitrogen concentration explain variation in canopy light use efficiency across 14 contrasting forest sites? *Tree Physiology* 32: 200–218.

Philip J.R. 1957. Evaporation, and moisture and heat fields in the soil. *Journal of Atmospheric Sciences* 14: 354–366.

Phillips N. & Oren R. 1998. A comparison of daily representations of canopy conductance based on two conditional time-averaging methods and the dependence of daily conductance on environmental factors. *Annals of Forest Science* 55: 217–235.

Pirinen P., Simola H., Aalto J., Kaukoranta J.P., Karlsson P. & Ruuhela R. 2012. *Tilastoja Suomen ilmastosta 1981–2010*. Ilmatieteen laitos, Helsinki.

Reichstein M., Falge E., Baldocchi D., Papale D., Aubinet M., Berbigier P., Bernhofer C., Buchmann N., Gilmanov T., Granier A., Grunwald T., Havrankova K., Ilvesniemi H., Janous D., Knohl A., Laurila T., Lohila A., Loustau D., Matteucci G., Meyers T., Miglietta F., Ourcival J.-M., Pumpanen J., Rambal S., Rotenberg E., Sanz M, Tenhunen J., Seufert G., Vaccari F., Vesala T., Yakir D. & Valentini R. 2005. On the separation of net ecosystem exchange into assimilation and ecosystem respiration: review and improved algorithm. *Global Change Biology* 11: 1424–1439.

Priestley C.H.B. & Taylor R.J. 1972. On the assessment of surface heat flux and evaporation using large-scale parameters. *Monthly Weather Review* 100: 81–82.

Rosenthal J.S. 2007. AMCMC: An R interface for adaptive MCMC. *Computational Statistics & Data Analysis* 51: 1–6.

Schulze E.-D., Leuning R. & Kelliher F.M. 1995. Environmental regulation of surface conductance for evaporation from vegetation. *Vegetatio* 121: 79–87.

Shaw S.B. & Riha S. 2011. Assessing temperature-based PET equations under a changing climate in temperate, deciduous forests. *Hydrological Processes* 25: 1466–1478.

Smith P., Smith J.U., Powlson D.S., McGill W.B., Arah J.R.M., Chertov O.G., Coleman K., Franko U., Frolk-

ing S., Jenkinson D.S., Jensen L.S., Kelly R.H., Klein-Gunnewiek H., Komarov A.S., Li C., Molina J.A.E., Mueller T., Parton W.J., Thornley J.H.M. & Whitmore A.P. 1997. A comparison of the performance of nine soil organic matter models using datasets from seven long-term experiments. *Geoderma* 81: 153–225.

Suni T., Rinne J., Reissell A., Altimir N., Keronen P., Rannik Ü., Dal Maso M., Kulmala M. & Vesala T. 2003. Long-term measurements of surface fluxes above a Scots pine forest in Hyytiala, southern Finland, 1996–2001. *Boreal Environment Research* 8: 287–301.

Thum T., Aalto T., Laurila T., Aurela M., Lindroth A. & Vesala T. 2008. Assessing seasonality of biochemical CO_2 exchange model parameters from micrometeorological flux observations at boreal coniferous forest. *Biogeosciences* 5: 1625–1639.

Turc L. 1961. Evaluation des besoins en eau d'irrigation. Evapotranspiration potentielle. *Annales agronomiques* 12: 13–49.

Whitehead D. 1998. Regulation of stomatal conductance and transpiration in forest canopies. *Tree Physiology* 18: 633–644.

Wu S.H., Jansson P. & Kolari P. 2011. Modeling seasonal course of carbon fluxes and evapotranspiration in response to low temperature and moisture in a boreal Scots pine ecosystem. *Ecological Modelling* 222: 3103–3119.